ELSEVIER

Chemical Physics 262 (2000) 243–252

Chemical Physics

www.elsevier.nl/locate/chemphys

Experimental and theoretical study of the reaction of the ethynyl radical with acetylene (HC≡C + HC≡CH)

Benny Ceursters, Hue Minh Thi Nguyen [1], Jozef Peeters, Minh Tho Nguyen *

Department of Chemistry, University of Leuven, Celestijnenlaan 200F, B-3001 Leuven, Belgium

Received 22 June 2000; in final form 25 September 2000

Abstract

The absolute rate coefficient of the reaction of the ethynyl radical with acetylene was measured using a pulsed laser photolysis/chemiluminescence (PLP/CL) technique in which HCC radicals were generated by excimer laser photodissociation of acetylene at 193 nm, and pseudo-first-order exponential decays of thermalized HCC were monitored in real time by the CH($A^2\Delta \rightarrow X^2\Pi$) CL resulting from their reaction with O_2. The rate coefficient as determined using this single, absolute technique over the extended temperature range of $295 \leqslant T$ (K) < 800 was found to exhibit no temperature dependence, the result being $k_{\text{acetylene}} = (1.3 \pm 0.1) \times 10^{-10}$ cm^3 molecule^{-1} s^{-1}. B3LYP and CCSD(T)/6-311++G(d,p) calculations revealed that while the direct H-abstraction has a barrier of $\approx$40 kJ mol^{-1}, the terminal C-addition is barrier-free giving the 2-ethynyl-vinyl radical (HC≡C–CH=CH) which either dissociates directly into diacetylene (HC≡C–C≡CH + H) or first rearranges to 1-ethynyl-vinyl (HC≡C–C=CH$_2$) before undergoing a H-loss. In both these pathways, all intermediates and transition structures lie energetically well below the reactants and therefore both fragmentation pathways are open to thermal reactants. An additional C_4H_2 + H forming pathway through the vinylidene HC=CH–CH=C was identified; it is expected to contribute at higher flame temperatures. © 2000 Published by Elsevier Science B.V.

1. Introduction

There has been considerable interest in the ethynyl radical (HCC), one of the primary products of the acetylene decomposition, in part owing to the importance of its reactions occurring in a wide variety of natural and man-made environments containing acetylene. Its electronic and spectroscopic properties have been investigated extensively [1,2]. The abundant presence of HCC in interstellar space and planetary atmospheres (such as Titan's) has stimulated recent studies of their low-temperature kinetics [3]. On earth, HCC plays an important role in the combustion reactions of fossil fuels and is invoked as a key precursor in the formation of diacetylene (C_4H_2) and the higher polyacetylenes ($C_{2n}H_n$), as well as of polycyclic aromatic hydrocarbons and hence of soot [4–12]. The fast reaction (1) is thus crucial in this respect:

$$\text{HC}{\equiv}\text{C} + \text{HC}{\equiv}\text{CH} \rightarrow \text{HC}{\equiv}\text{C–C}{\equiv}\text{CH} + \text{H}, \quad \Delta H_r(0\ \text{K}) = -109\,\text{kJ mol}^{-1} \qquad (1)$$

* Corresponding author.

E-mail addresses: jozef.peeters@chem.kuleuven.ac.be (J. Peeters), minh.nguyen@chem.kuleuven.ac.be (M.T. Nguyen).

[1] On leave from Faculty of Chemistry, National University of Education, Hanoi, Vietnam.

0301-0104/00/$ - see front matter © 2000 Published by Elsevier Science B.V.
PII: S0301-0104(00)00337-2

In fuel-rich near-sooting hydrocarbon flames, the fraction of primary fuel that passes through C_4H_2 can amount to more than 50% [6,7]. Ethynyl radicals also react fast with NO yielding primarily HCN and CO [13–16] and as such, they may intervene in NO_x chemistry in conditions where C_2H is an important intermediate, i.e. in fuel-rich hydrocarbon flames in general and in high-temperature "NO-reburning" [17,18] in particular.

In this regard, detailed and quantitative information on the mechanism and kinetics of formation and destruction of HCC by small radicals and molecules over a broad-temperature range is of fundamental chemical importance.

The present work focuses on the reaction of HCC with acetylene. The kinetics of HCC + HCCH have been studied by a number of authors using different experimental approaches [19–28,30]. A synopsis of the earlier work can be found in Ref. [30]. Although most of the recent measurements [19–25,30] agree on a 300 K rate constant value of $k_{\text{acetylene}} = (1.4 \pm 0.2) \times 10^{-10}$ $\text{cm}^3\,\text{molecule}^{-1}\,\text{s}^{-1}$, the temperature dependence of the rate coefficient is still in doubt [20–24] (see Fig. 3). At higher temperatures (295–2000 K), the $k_{\text{acetylene}}$ data obtained indirectly [20–22] show a slight positive T dependence, while the absolute, direct measurements [24] on the other hand indicate a negative T dependence of the rate coefficient. At lower temperatures (170–350 K), the results show that $k_{\text{acetylene}}$ is quasi-independent of temperature [23]. Hence, the temperature dependence of the kinetic coefficient for $T > 300$ K must be established precisely, preferably using one and the same absolute, direct technique over a wide temperature region. Furthermore, although diacetylene is generally accepted to be the primary product of the HCC + HCCH reaction, its detailed formation mechanism is still not well established. A reaction pathway computed using MO calculations, along with a theoretical study of chemical dynamics at low temperatures, was reported recently [29]. Nevertheless, only one intermediate was considered for the addition–dissociation route.

As part of our continuing study of the gas phase reactions of HCC [13–16,30–33], we set out to reinvestigate in the present work the reactivity of ethynyl radicals toward acetylene using both experimental and theoretical approaches. Absolute bimolecular rate coefficients have been determined over the 295–800 K temperature domain using a pulsed laser photolysis/chemiluminescence (PLP/CL) technique. This technique as developed by us was validated earlier as a very precise and highly accurate tool for investigating the gas-phase kinetics of the HCC radical, both for barrier-free reactions [30] and reactions with an appreciable energy barrier [31,32]. In addition, the experimental study was supplemented by ab initio quantum chemical calculations of possible reaction intermediates and their decomposition that thus allow the formation mechanism(s) of diacetylene to be identified.

2. Experimental results

The instrumental arrangement used in the PLP/CL experiments is similar to that employed in our earlier studies of HCC kinetics [13–15,30–32]. It is part of a PLP/LIF setup described in detail previously [34,35]. Therefore, only the main characteristics will be briefly mentioned here.

Ethynyl radicals were generated by continuously flowing a gas mixture of acetylene, molecular oxygen and helium into a reaction cell and photolyzing the C_2H_2 by a 193 nm pulsed ArF excimer laser (30 mJ pulse^{-1} at 10 Hz, beam section of 8×3 mm^2). The real-time pseudo-first-order decay of HCC was monitored by measuring the intensity $I(\text{CH}^*)$ of the 430 nm $\text{CH}(\text{A}^2\Delta \rightarrow \text{X}^2\Pi)$ CL [31,32] resulting from the reaction of HCC with O_2, present in a large and constant concentration (reaction (2)) [30]:

$$\begin{aligned} \text{HCC} + \text{O}_2 &\rightarrow \text{products} \\ &\rightarrow \text{CO}_2 + \text{CH}(\text{A}^2\Delta) \qquad (2) \\ \text{CH}(\text{A}^2\Delta) &\rightarrow \text{CH}(\text{X}^2\Pi) + h\nu\ (430\ \text{nm}) \end{aligned}$$

Under the experimental conditions, $I(\text{CH}^*)$ is directly proportional to the ethynyl concentration. The CL perpendicular to the laser beam is collected through a lens, and focused through an interference filter ($\lambda_{\max} = 430$ nm; FWHM = 10 nm) on a photomultiplier tube, the signals of which are

processed by a boxcar integrator. The delay between firing the laser and opening the 1 μs boxcar gate was increased after each photolysis pulse at a rate of 0.1 $\mu s\,s^{-1}$. The reaction cell in this work was equipped with an inner ceramic tube with a Ni/Cr resistive wire coil, to heat the (slowly) flowing gas mixture up to 800 K. The temperature in the small observed reaction volume ($8 \times 3 \times 10$ mm^3) at the center of the tube was measured by a movable calibrated chromel/alumel thermocouple. Oxygen (99.995%) and helium (99.9990%) were used as received commercially (both AIR LIQUIDE); acetylene (99.5%, HOEK LOOS) was passed through a dry ice/acetone trap to remove the acetone. Acetylene and molecular oxygen were always present in a very large excess over HCC (initial ethynyl concentration $\approx 10^{12}$ molecules cm^{-3}), such that contributions from secondary and/or radical–radical reactions are negligible. Transport of the HCC out of the observed volume by diffusion or convection, on a time scale of several ms, cannot compete with chemical reaction losses occurring on a μs time scale. Since pseudo-first-order conditions obtain, one then has:

$$[HCC]_t = [HCC]_0 \exp(-k't) \tag{3}$$

where

$$k' = k_{acetylene}[C_2H_2] + k_{oxygen}[O_2]. \tag{4}$$

The total bath gas pressure of 10 Torr He and the oxygen number densities $[O_2] \geqslant 4.6 \times 10^{15}$ molecules cm^{-3} ensure thermalization of the HCC within the 5 μs period prior to the decay measurements, as ascertained earlier [30]. An example of a HCC exponential decay is shown in Fig. 1. Rate coefficients $k_{acetylene}$ of the reaction of HCC with acetylene were determined by measuring the first-order decay constant k' at varying $[O_2]$ and at fixed $[C_2H_2]$. The slope of the linear plot of k' vs. $[O_2]$ yields the bimolecular rate coefficient k_{oxygen}, whereas the ordinate intercept is equal to $k_{acetylene}[C_2H_2]$. A typical example of a plot of k' as a function of $[O_2]$ at fixed $[C_2H_2]$ is given in Fig. 2. The present $k_{acetylene}$ results in the range $T =$ 448–777 K, obtained by the intercept method, are given in Table 1, together with the results obtained earlier in this laboratory [30] in a similar manner

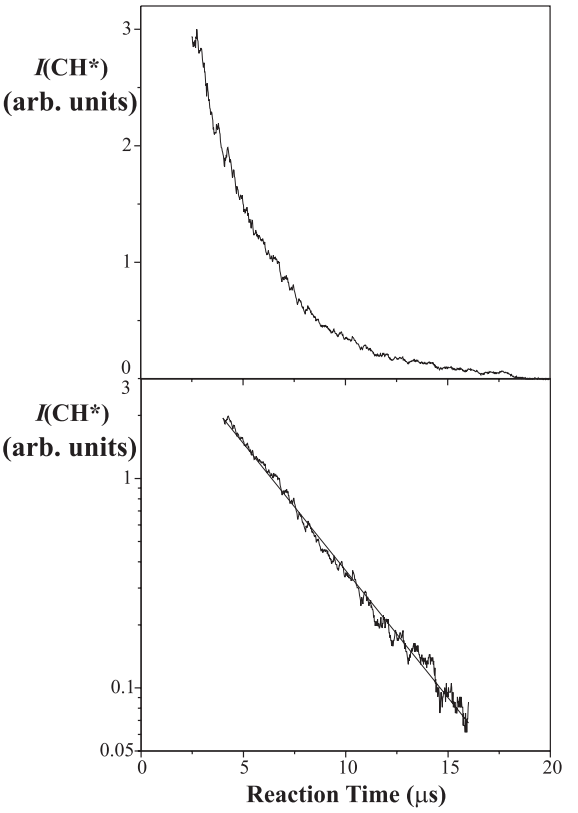

Fig. 1. Typical decay and semilog plot of the relative HCC concentration vs. reaction time; $T = 689$ K; $p_{tot} = 10$ Torr (He bath gas); $[C_2H_2] = 4.63 \times 10^{14}$ molecules cm^{-3}. The straight line represents the weighted linear least-squares fit.

over the temperature range of $T =$ 295–448 K. To check for possible systematic errors, the $k_{acetylene}$(448 K) result was remeasured and was reproduced exactly. It should be noted that in our previous work determinations of $k_{acetylene}$ were also made in the conventional way, i.e. from the slope of k' vs. $[C_2H_2]$ plots at a constant $[O_2]$, yielding $k_{acetylene}$ values identical to that obtained by the intercept method [30]. The average precision on the results obtained by the intercept method, of 4%, is similar to the precision of 2–5% by the conventional method. The quality of data obtained by the intercept method can also be assessed from the following. In rate coefficient measurements of other C_2H reactions, e.g. with CH_4 [13–15], first-order decay constants k' are measured for varying $[CH_4]$ but at fixed $[C_2H_2]$ as well as

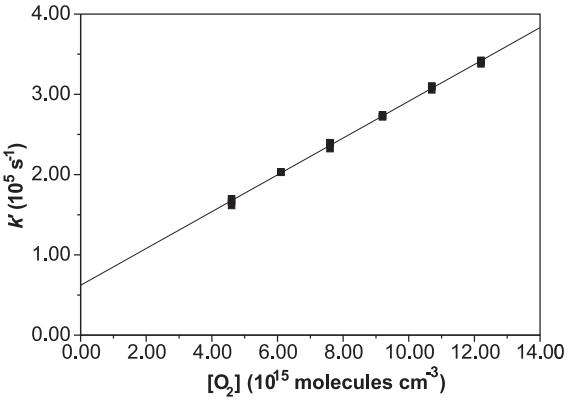

Fig. 2. Pseudo-first-order rate constants k' plotted vs. $[O_2]$ at $T = 777$ K; $p_{tot} = 10$ Torr (He bath gas); $[C_2H_2] = 4.55 \times 10^{14}$ molecules cm^{-3}. The solid line represents a weighted linear least-squares fit to the data points. The gradient of the line yields $k_{oxygen}(777\ K) = (2.31 \pm 0.23) \times 10^{-11}$ cm^3 molecule^{-1} s^{-1}. The ordinate intercept is equal to $k_{acetylene}[C_2H_2] = (6.05 \pm 0.21) \times 10^4$ s^{-1}, implying a value of $k_{acetylene}(777\ K) = (1.33 \pm 0.13) \times 10^{-10}$ cm^3 molecule^{-1} s^{-1}.

Table 1
Bimolecular rate coefficients $k_{acetylene}$ (in cm^3 molecule^{-1} s^{-1}) for the reaction of HCC with C_2H_2 over the range $T = 295$–777 K and at a pressure of 10 Torr He derived from the intercept values of k' vs. $[O_2]$ plots

T (K)	1000/T (K^{-1})	$k_{C_2H_2} \times 10^{10}$	Reference
295	3.39	1.33 ± 0.20	[30]
332	3.01	1.34 ± 0.13	[30]
366	2.73	1.33 ± 0.13	[30]
393	2.55	1.31 ± 0.13	[30]
448	2.23	1.34 ± 0.13	[30]
448	2.23	1.39 ± 0.14	This work
528	1.89	1.22 ± 0.12	This work
601	1.66	1.20 ± 0.12	This work
689	1.45	1.33 ± 0.13	This work
777	1.29	1.33 ± 0.13	This work

$[O_2]$; the intercepts obtained are in all cases identical within 2% to the sum $k_{acetylene}[C_2H_2] + k_{oxygen}(T)[O_2]$ with $k_{acetylene} = 1.3 \times 10^{-10}$ as measured in the present work and $k_{oxygen}(T) = 1.96 \times 10^{-11}$ exp(150 K/T) cm^3 molecule^{-1} s^{-1} as determined separately [13–15,30].

The full set of $k_{acetylene}$ data in the T-range of 295–800 K (Table 1) shows no definite temperature dependence. The average $k_{acetylene}$ value amounts to $(1.3 \pm 0.1) \times 10^{-10}$ cm^3 molecule^{-1} s^{-1}.

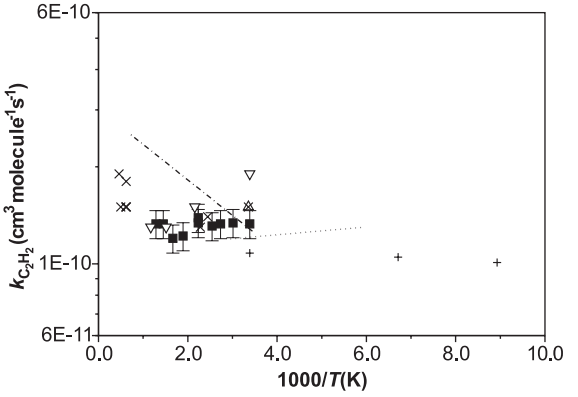

Fig. 3. Arrhenius plot showing the rate coefficient for the gas phase reaction HCC + C_2H_2: (■) 450–800 K: this work; (■) 295–450 K: Ref. [30]; (△) Ref. [19]; (-·-·-) Ref. [20]; (×) Refs. [21,22]; (···) Ref. [23]; (▽) Ref. [24]; (+) Ref. [25]. Error bars for our results (■) include possible systematic errors.

Fig. 3 shows an Arrhenius representation of the $k_{acetylene}$ determinations of this laboratory along with the results previously reported by other groups [19–25]. The early results of Lange and Wagner [26] and Laufer and Bass [27] were not included here since the rate constant of the former was only a lower limit and that of the latter was determined in an indirect way. Note that Lange and Wagner [26] reported traces of C_4H_3 radicals. It can be seen that our result $k_{acetylene}(295\ K) = (1.33 \pm 0.20) \times 10^{-10}$ cm^3 molecule^{-1} s^{-1}, reported in our earlier paper [30], is in close agreement with the more recent literature data at this temperature. Both Shin and Michael [20] and Pedersen et al. [23] also obtained a value of 1.3×10^{-10} cm^3 molecule^{-1} s^{-1}. Stephens et al. [19] as well as Koshi et al. [21,22] derived a rate constant of 1.5×10^{-10} cm^3 molecule^{-1} s^{-1} at room temperature, whereas the result reported by Farhat et al. [24] is slightly higher, viz. 1.9×10^{-10} cm^3 molecule^{-1} s^{-1}. More recently, Chastaing et al. [25] obtained a value of 1.08×10^{-10} cm^3 molecule^{-1} s^{-1}, which is somewhat lower than the other data.

Our finding of a T-independent $k_{acetylene}$ in the 300–800 K range is in line with the likewise absolute determinations of Pedersen et al. [23] for the range 170–300 K, although their values are slightly lower. Shin and Michael [20], using a different

technique at 1228–1475 K from that at 298 K, found a positive T-dependence; however, given the substantial uncertainty on their high-T data, the authors note that a T-dependence of the rate coefficient is not certain.

3. Quantum chemical calculations

Having established the rate constant of the $HCC + C_2H_2$ reaction, we now attempt to identify the most likely product channels using ab initio quantum chemical calculations. The (C_4H_3) system contains several low-energy isomers including the 2-ethynyl-vinyl (HC≡C–CH=CH) and 1-ethynyl-vinyl (HC≡C–C=CH_2) and a number of cyclic radicals. It is not our intention here to explore fully this interesting potential energy surface. Our search was rather limited to the part of the energy surface comprising the reaction pathways starting from $HCC + C_2H_2$ and leading to diacetylene (HC≡C–C≡CH + H). Thus we were not searching for the connections between the possible intermediates unless they are relevant to the product formation. For example, although the $HCCCC + H_2$ fragments are a low-energy isomer and directly connected to HCCCCH + H via a H-abstraction, we were not able, in spite of intensive search, to locate a transition structure connecting them to one of the C_4H_3 adducts; therefore this channel is not considered.

All calculations were performed using the GAUSSIAN 94 suite of programs [36]. Geometry optimizations were conducted using molecular orbital theory at the Hartree–Fock (HF), second-order perturbation theory (MP2) and density functional theory with the popular hybrid functional B3LYP, in conjunction with the 6-311++G(d,p) basis set. Electronic energies at the coupled-cluster theory level with all single and double excitations plus perturbative corrections for triple substitutions (CCSD(T)) were further computed using B3LYP optimized geometries. The unrestricted formalism (UHF, UMP2 and UCCSD) was used for open-shell states. Harmonic vibrational wave numbers were calculated at both UHF and UB3LYP level to characterize the stationary points as equilibrium and transition structures. The zero-point energies (ZPE) were derived from UB3LYP frequencies scaled down by a uniform factor of 0.97. In (U)MP2 and (U)CCSD(T) calculations, the core orbitals were kept frozen. Due to the presence of two multiple bond systems, the UHF wave functions for doublet states are heavily spin-contaminated with large expectation values for $\langle S^2\rangle \geqslant 1.0$. Therefore the UHF and UMP2 energies and parameters need to be regarded with much caution, in particular the UMP2 values that are subject to the effect of slow convergence of the MP perturbation series. In this regard, the B3LYP method is seemingly more appropriate for investigating this radical system. Nevertheless, this method is known to have some shortcomings in treating the addition/elimination of the hydrogen atom [37]. Therefore, geometries of the relevant transition structures were reoptimized using CCSD(T) calculations in order to verify the validity of B3LYP parameters.

While Fig. 4 displays the selected B3LYP/6-311++G(d,p) geometrical parameters of the relevant stationary points, Table 2 summarizes the calculated relative energies. Schematic potential energy profiles showing the different pathways are illustrated in Fig. 5. In general, the ordering of relative energies obtained by both B3LYP and CCSD(T) methods is similar; there are some differences in the absolute relative energies here and there. It appears that the B3LYP treatment tends to significantly enlarge the energy differences between (C_4H_3) stationary points, up to 40 kJ mol^{-1}, relative to the starting $HCC + C_2H_2$ system. Unless stated otherwise, we use the CCSD(T)//B3LYP + ZPE relative energies for the discussion hereafter. Throughout this section, bond lengths are given in angstrom, bond angles in degree, total energies in hartree, relative and ZPE in kJ mol^{-1}.

The ethynyl radical exhibits a $^2\Sigma^+$ electronic ground state in which the unpaired electron is mainly located in the 2p(σ) orbital of the terminal carbon atom. Upon bending, a certain amount of the unpaired electron is actually transferred to the central carbon in such a way that the latter could also act as a radical center. Due to the fact that the bending of HCC is a quite facile motion with an experimental vibrational frequency of only 371 cm^{-1} [38], both carbon atoms of HCC could

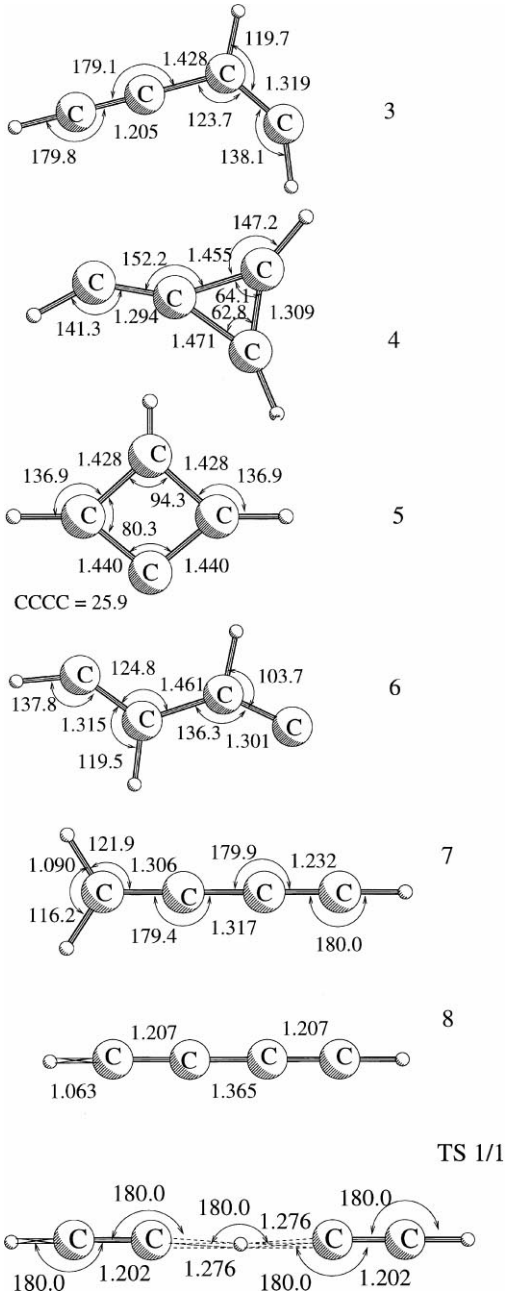

Fig. 4. Selected B3LYP/6-311++G(d,p)-optimized geometrical parameters of the stationary points related to the HCC + C_2H_2 reaction. Distances are given in Å and bond angles in degrees.

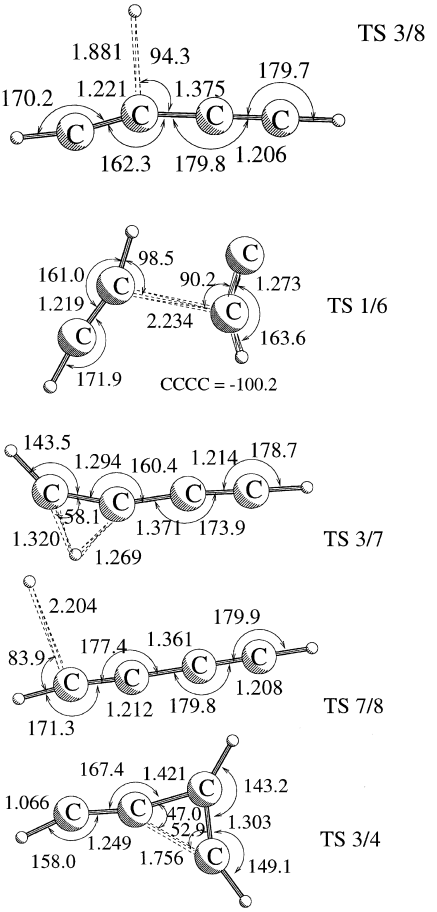

Fig. 4 (*continued*)

behave as reactive radical sites. A priori, each radical center could either abstract a hydrogen of acetylene, or insert into one of its C–H bonds or add to the triple C≡C bond. Starting from the HCC + HCCH reactants **1**, only one transition structure for hydrogen abstraction TS **1/1** has been located which is a symmetrical TS for a degenerate reaction, with rather short C···H distances (1.28 Å). Starting from the vinylidene isomer (H_2CC + HCC **2**), no TS for H-abstraction vinylidene could be found, due no doubt to the higher energy of vinylidene which lies 177 kJ mol^{-1} above acetylene. The H-abstraction via TS **1/1** requires to overcome a significant energy barrier of about 46 kJ mol^{-1}.

For the radical addition of HCC to the triple bond of acetylene, there are in principle three distinct avenues: (i) a direct attack giving the 1-ethynyl-vinyl radical **3**, (ii) a [2 + 1] addition giving the three-membered ring **4**, and (iii) a [2 + 2]

Table 2
Calculated relative energies (in kJ mol^{-1}) of the (C_4H_3) stationary points considered at two levels of theory

Structure		B3LYP[a] 6-311++G(d,p)	CCSD(T)[b] 6-311++G(d,p)	ZPE[c]
HCC + HCCH	**1**	0	0	105
HCC + H_2CC	**2**	170	177	95
HC≡C–CH=CH	**3**	−262	−239	120
3-ring	**4**	−179	−147	112
4-ring	**5**	−151	−130	120
C=CH–CH=CH	**6**	−74	−55	113
HC≡C–C=CH_2	**7**	−333	−295	115
HCCCCH + H	**8**	−129	−110	96
TS	**1/1**	27	46	93
TS	**1/6**	8	32	107
TS	**3/3**	−248	−219	115
TS	**3/4**	−157	−123	112
TS	**3/7**	−98	−65	102
TS	**3/8**	−106	−73	98
TS	**7/8**	−124	−98	97

[a] Relative energies including ZPE corrections. The B3LYP/6-311++G(d,p) total energy is **1**: −153.98761 hartree.
[b] Relative energies including ZPE corrections. The CCSD(T)/6-311++G(d,p) total energy is **1**: −153.56643 hartree.
[c] Zero-point vibrational energies, in kJ mol^{-1}, obtained from B3LYP/6-311++G(d,p) frequencies and scaled down by 0.97.

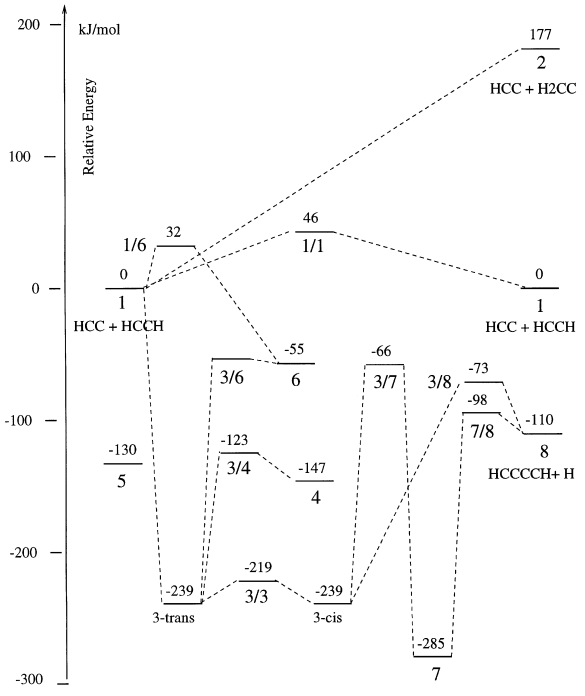

Fig. 5. Schematic potential energy profiles (kJ mol^{-1}) illustrating the different pathways of the HCC + C_2H_2 reaction. Relative energies given are obtained from CCSD(T)/6-311++G(d,p) + ZPE computations.

addition giving the four-membered ring **5**. It turns out that the open radical **3** is far more stable than the cyclic isomers **4** and **5**. Our results concur with earlier findings [29] that the addition **1** yielding **3** is a barrier-free process. While the three-membered ring **4**, a radical of fulvene, has a planar form, the cycle **5**, a radical of cyclobutadiene, features a puckered four-membered ring. The cycle **4** can easily rearrange into the more stable open form **3** via TS **3/4** which lies only 24 kJ mol^{-1} above **4**.

For its part, the radical **6** formally results from an addition of the HCC central carbon to an acetylene carbon; the corresponding process through TS **1/6** is characterized by an energy barrier of 32 kJ mol^{-1}. It is worth noting that **1/6** lies somewhat lower in energy than TS **1/1**. Both forms **3** and **6** are formally connected to each other by a acetylene and vinylidene relationship. Although a TS **3/6** has been found at the HF level, we have encountered difficulties, in spite of extensive attempts, in locating this TS at the B3LYP level. In order to have a rough estimate of its relative energy level, we have used its UHF geometry and carried out single-point electronic energy at the CCSD(T) level. The calculated results indicate that TS **3/6** is expected to lie only a few kJ mol^{-1}

above **6**, and as a consequence, the vinylidene **6** is a quite unstable form. Nevertheless, this route also leading to the formation of the product, could contribute to the global rate at higher temperatures. Because of its rather high energy content and the lack of direct and obvious connections to the product, the form **5** will not be considered further here.

The 2-ethynyl-vinyl adduct radical **3** is calculated to lie about 239 kJ mol^{-1} below the reactants **1**. This value compares quite well with that of 237 kJ mol^{-1} obtained earlier using CCSD(T)/cc-pVTZ + ZPE computations based on CCSD(T)/cc-pVDZ optimized geometries [29]. The radical **3** can exist in *trans* and *cis* having equal energies; both isomers are connected to each other by the TS for inversion **3/3** around the vinyl carbon and characterized by an energy barrier of about 20 kJ mol^{-1}. Starting from **3**, two distinct product channels are open including: (i) a hydrogen loss via TS **3/8** directly producing HCCCCH + H **8** and (ii) an initial rearrangement to 1-ethynyl-vinyl **7** involving the TS for 1,2-H shift **3/7** followed by a hydrogen loss from the latter via TS **7/8**. The radical isomer **7** turns out to be about 46 kJ mol^{-1} more stable than **3**. In the latter route (ii), the difficult step is actually the 1,2-H shift whose TS **3/8** lies about 166 kJ mol^{-1} above **3**. Owing to the lower potential energy of **7** relative to **3**, the TS **7/8** for H-elimination is lower in energy than the corresponding **3/8** by about 25 kJ mol^{-1}. This energy difference between both TS's **3/8** and **7/8** can be understood in proceeding in the opposite direction, namely the hydrogen addition to diacetylene. This addition reaction is mainly controlled by the interaction between the frontier orbitals SOMO(H) and LUMO(HCCCCH). In the latter orbital, the terminal carbon atoms possess larger 2pπ-orbital lobes than the central ones, and therefore they involve larger stabilization energies resulting in a smaller energy barrier for hydrogen addition. In other words, the TS **7/8** is expected to lie lower in energy than the **3/8** counterparts. Perhaps a more important aspect of the energy surface is that all intermediates and transition structures for 1,2-H shifts and H-losses are found to lie *below the reactants*. In this regard, both product channels seen in Fig. 5 are probably open but with different contributions to the diacetylene formation. In an earlier study, Brachhold et al. [28] estimated a life time of 7.4×10^{-11} s for the activated adduct $\mathbf{3}^{\neq}$ using a crude RRKM treatment considering only this intermediate. Although this estimate is seemingly not quite accurate in view of the present results showing a possible formation of a more stable intermediate, the extremely short-lived complex is not inconsistent with the fact that no pressure dependence was apparent in the investigated range of 10–100 Torr [23]. On the other hand, energetic results shown in Fig. 5 indicate that it is appropriate to consider both product channels in further RRKM analyses of the product formation.

It is worthwhile to note that for both TS's **3/8** and **7/8** for addition/elimination of hydrogen, the B3LYP method provides with quite reasonable inter-fragment C···H distances. For example, the B3LYP value of 1.889 Å in TS **3/8** is only slightly longer than the CCSD(T) counterpart of 1.825 Å. Indeed, much larger differences (much longer B3LYP values) could usually be expected for this type of reactions [37]. On the other hand, the energy surface in this region is rather flat, implying that a large change in the C···H distance induces only a small variation in relative energies. As far as the hydrogen abstraction reaction is concerned, we note that there are actually some conflicting views [39,40] regarding the validity of various quantum chemical methods. Here we found that for TS **1/1**, both B3LYP and CCSD(T) approaches result in comparable geometry parameters.

4. Concluding remarks

In the present study of the gas phase reaction of the ethynyl radical with acetylene making use of both experimental kinetic and quantum chemical methods, the temperature dependence of the $k_{\text{acetylene}}$ rate coefficient was investigated over the temperature range of $295 \leqslant T\ (\text{K}) < 800$. The rate coefficient as determined using one and the same absolute technique, shows no temperature dependence. The result of $k_{\text{acetylene}} = (1.3 \pm 0.1) \times 10^{-10}$

$cm^3\,molecule^{-1}\,s^{-1}$ is near the average of other recent determinations. B3LYP and CCSD(T)/6-311++G(d,p) calculations revealed that while the direct H-abstraction faces a barrier of ≈40–45 $kJ\,mol^{-1}$, the addition of the HCC terminal carbon is barrier-free forming the 2-ethynyl-vinyl radical (HC≡C–CH=CH) which either dissociates directly into diacetylene (HC≡C–C≡CH + H) or first rearranges to 1-ethynyl-vinyl (HC≡C–C=CH_2) before undergoing a H-loss. Although the 1,2-H shift linking both isomeric radicals is characterized by a larger barrier height than those for H-elimination, all intermediates and transition structures are energetically situated below the reactants and therefore both product formation channels are expected to be open and need to be included in any kinetic treatment. An additional C_4H_2 + H forming pathway, via the vinylidene derivative HC=CH–CH=C, was identified; it faces an entrance barrier of about 32 $kJ\,mol^{-1}$ and is therefore expected to become important at higher flame temperatures.

Acknowledgements

The authors are indebted to the Fund for Scientific Research (FWO-Vlaanderen) and KULeuven Research Council for continuing support.

References

[1] W.Y. Chiang, Y.C. Hsu, J. Chem. Phys. 111 (1999) 1454 (and references therein).
[2] M. Boggio-Pasqua, A.I. Voronin, Ph. Halvick, J.C. Rayez, J. Phys. Chem. Chem. Phys. 2 (2000) 1693 (and references therein).
[3] R.J. Hoobler, S.R. Leone, J. Phys. Chem. A 103 (1999) 1342 (and references therein).
[4] U. Bonne, K.H. Homann, H.Gg. Wagner, Symp. (Int.) Combust. [Proc.] 10 (1965) 503.
[5] J.D. Bittner, J.B. Howard, Symp. (Int.) Combust. [Proc.] 19 (1982) 211.
[6] J. Warnatz, Combust. Sci. Technol. 34 (1983) 177.
[7] J. Warnatz, Ber. Bunsenges. Phys. Chem. 87 (1983) 1008.
[8] H. Bockhorn, F. Fetting, H.W. Wenz, Ber. Bunsenges. Phys. Chem. 87 (1983) 1067.
[9] J.A. Kiefer, W.A. Von Drasek, Int. J. Chem. Kinet. 22 (1990) 747.
[10] R.P. Lindstedt, G. Skevis, Combust. Sci. Technol. 125 (1997) 73.
[11] C. Douté, J.-L. Delfau, C. Vovelle, Combust. Sci. Technol. 103 (1994) 153.
[12] M. Frenklach, H. Wang, Symp. (Int.) Combust. [Proc.] 23 (1990) 1559.
[13] J. Peeters, H. Van Look, B. Ceursters, J. Phys. Chem. 100 (1996) 15124.
[14] B. Ceursters, Ph.D. Thesis, K.U. Leuven 2000.
[15] B. Ceursters, H.M.T. Nguyen, J. Peeters, M.T. Nguyen, Chem. Phys. Lett., in press.
[16] D. Sengupta, J. Peeters, M.T. Nguyen, Chem. Phys. Lett. 91 (1998) 283.
[17] J.A. Miller, C.T. Bowman, Prog. Energy Combust. Sci. 15 (1989) 287.
[18] C.T. Bowman, Symp. (Int.) Combust. [Proc.] 24 (1992) 859.
[19] J.W. Stephens, J.L. Hall, H. Solka, W.-B. Yan, R.F. Curl, G.P. Glass, J. Phys. Chem. 91 (1987) 5740.
[20] K.S. Shin, J.V. Michael, J. Phys. Chem. 95 (1991) 5864.
[21] M. Koshi, N. Nishida, H. Matsui, J. Phys. Chem. 96 (1992) 5875.
[22] M. Koshi, K. Fukuda, K. Kamiya, H. Matsui, J. Phys. Chem. 96 (1992) 9839.
[23] J.O.P. Pedersen, B.J. Opansky, S.R. Leone, J. Phys. Chem. 97 (1993) 6822.
[24] S.K. Farhat, C.L. Morter, G.P. Glass, J. Phys. Chem. 97 (1993) 12789.
[25] D. Chastaing, P.L. James, I.R. Sims, I.W.M. Smith, Faraday Discuss. 109 (1998) 165.
[26] W. Lange, H.Gg. Wagner, Ber. Bunsenges. Phys. Chem. 79 (1975) 165.
[27] A.H. Laufer, A.M. Bass, J. Phys. Chem. 83 (1979) 310.
[28] H. Brachhold, U. Alkemade, K.H. Homann, Ber. Bunsenges. Phys. Chem. 92 (1988) 916.
[29] E. Herbst, D.E. Woon, Astrophys. J. 489 (1997) 109.
[30] H. Van Look, J. Peeters, J. Phys. Chem. 99 (1995) 16284.
[31] K. Devriendt, H. Van Look, B. Ceursters, J. Peeters, Chem. Phys. Lett. 261 (1996) 450.
[32] K. Devriendt, J. Peeters, J. Phys. Chem. A 101 (1997) 2546.
[33] R. Sumathi, J. Peeters, M.T. Nguyen, Chem. Phys. Lett. 287 (1998) 109.
[34] J. Peeters, S. Vanhaelemeersch, J. Van Hoeymissen, R. Borms, D. Vermeylen, J. Phys. Chem. 93 (1989) 3892.
[35] J. Peeters, J. Van Hoeymissen, S. Vanhaelemeersch, D. Vermeylen, J. Phys. Chem. 96 (1992) 1257.
[36] M.J. Frisch, G.W. Trucks, H.B. Schlegel, P.M.W. Gill, B.G. Johnson, M.A. Robb, J.R. Cheeseman, T. Keith, G.A. Petersson, J.A. Montgomery, K. Raghavachari, M.A. Al-Laham, V.G. Zakrzewski, J.V. Ortiz, J.B. Foresman, J. Cioslowski, B.B. Stefanov, A. Nanayakkara, M. Challacombe, C.Y. Peng, P.Y. Ayala, W. Chen, M.W. Wong, J.L. Andres, E.S. Replogle, R. Gomperts, R.L. Martin, D.J. Fox, J.S. Binkley, D.J. DeFrees, J. Baker, J.J.P. Stewart, M. Head-Gordon, C. Gonzalez, J.A. Pople, GAUSSIAN 94, Revision E.2, Gaussian Inc., Pittsburgh PA, 1995.

[37] M.T. Nguyen, S. Creve, L.G. Vanquickenborne, J. Phys. Chem. 101 (1996) 18422.
[38] H. Kanamori, E. Hirota, J. Chem. Phys. 89 (1988) 3962.
[39] Y. Kobayashi, M. Kamiya, K. Hirao, Chem. Phys. Lett. 319 (2000) 695.
[40] R.G. Susnow, A.M. Dean, W.H. Green, Chem. Phys. Lett. 312 (1999) 262.